Journal of Zhejiang University-SCIENCE C (Computers & Electronics)
ISSN 1869-1951 (Print); ISSN 1869-196X (Online)
www.zju.edu.cn/jzus; www.springerlink.com
E-mail: jzus@zju.edu.cn

Numerical solutions of a multi-class traffic flow model on an inhomogeneous highway using a high-resolution relaxed scheme*

Jian-zhong CHEN†[1], Zhong-ke SHI[1], Yan-mei HU[2]

([1]*College of Automation, Northwestern Polytechnical University, Xi'an 710072, China*)

([2]*College of Science, Chang'an University, Xi'an 710064, China*)

†E-mail: jzhchen@nwpu.edu.cn

Received Sept. 16, 2010; Revision accepted Feb. 16, 2011; Crosschecked Dec. 5, 2011

Abstract: A high-resolution relaxed scheme which requires little information of the eigenstructure is presented for the multi-class Lighthill-Whitham-Richards (LWR) model on an inhomogeneous highway. The scheme needs only an estimate of the upper boundary of the maximum of absolute eigenvalues. It is based on incorporating an improved fifth-order weighted essentially non-oscillatory (WENO) reconstruction with relaxation approximation. The scheme benefits from the simplicity of relaxed schemes in that it requires no exact or approximate Riemann solvers and no projection along characteristic directions. The effectiveness of our method is demonstrated in several numerical examples.

Key words: Relaxed scheme, Multi-class model, Weighted essentially non-oscillatory (WENO) reconstruction
doi:10.1631/jzus.C10a0406 **Document code:** A **CLC number:** TP39; U49

1 Introduction

The Lighthill-Whitham-Richards (LWR) model (Lighthill and Whitham, 1955; Richards, 1956) was derived to describe the characteristics of traffic flow. Although it is simple, it can be used to explain a variety of real traffic phenomena such as shock formation. However, it fails to describe some important traffic phenomena, for instance, hysteresis of traffic flow, the dispersion of platoons, and the two-capacity phenomenon. To overcome these drawbacks, attempts have been made to extend the LWR model. A multi-class LWR (MCLWR) model with heterogeneous drivers (Wong and Wong, 2002) was found to remedy the above deficiencies of the LWR model. The MCLWR model was extended to deal with inhomogeneous road conditions (Zhang *et al*., 2006b) and was investigated for use in traffic network operations (Ngoduy, 2010).

Recently, high-order and high-resolution numerical schemes developed in the field of computational fluid mechanics have been gradually generalized to the MCLWR model. The weighted essentially non-oscillatory (WENO) scheme has been applied to the MCLWR model with heterogeneous drivers (Zhang *et al*., 2003) and the MCLWR model on an inhomogeneous highway (Zhang *et al*., 2006b). A hybrid scheme was presented for the MCLWR model for an inhomogeneous highway (Zhang *et al*., 2008). A relaxation scheme for the MCLWR model with heterogeneous drivers was introduced by Chen *et al*. (2009). The multi-class traffic flow model also belongs to kinematic models. A family of numerical schemes was proposed for kinematic flows with discontinuous flux by Bürger *et al*. (2008). The main advantage of the high-order, high-resolution schemes is that they can reduce the excessive numerical dissipation and produce much sharper resolution of discontinuities. Moreover, high-order schemes need fewer grid points to obtain the desired resolution and accuracy.

* Project supported by the National Natural Science Foundation of China (No. 11102165) and the Special Fund for Basic Scientific Research of Central Colleges, Chang'an University, China (No. CHD 2011JC039)

In this paper we are concerned mainly with relaxed schemes. First- and second-order relaxed schemes were first proposed by Jin and Xin (1995) and a third-order relaxed scheme with more precise information was introduced by Banda (2005). Banda (2009) applied a second-order relaxed scheme to one-dimensional ideal magnetohydrodynamic (MHD) equations. These relaxed schemes are the limit of the relaxation schemes as the relaxation rate tends to zero. Higher-order relaxation schemes have been suggested in the literature (Banda and Seaïd, 2005; 2007; Chen and Shi, 2006). The relaxed schemes are independent of the small relaxation rate and the artificial variables, and are stable discretizations of the original systems. The results computed by relaxed schemes are better than the corresponding results of relaxation schemes. Moreover, the relaxed schemes are less expensive.

The main advantage of relaxed schemes is that they do not need to employ Riemann solvers or characteristic decomposition. In fact, even the computation of the eigenvalues is not required. These features make relaxed schemes particularly suited for solving the MCLWR model, in which it is not possible to obtain an analytical expression for the eigenvalues of the Jacobians for more than two vehicular species.

In this work we combine a relaxed scheme with an improved fifth-order WENO reconstruction (Borges *et al*., 2008), and the third-order strong stability preserving (SSP) Runge-Kutta method (Gottlieb *et al*., 2001). The resulting high-resolution scheme is applied to the MCLWR model on an inhomogeneous highway. The numerical results show that our scheme has high accuracy and high-resolution properties.

2 The multi-class Lighthill-Whitham-Richards model

The MCLWR model on an inhomogeneous highway (Zhang *et al*., 2006b) can be written in conservation form as

$$\boldsymbol{u}_t+\boldsymbol{f}(\boldsymbol{u}, \boldsymbol{\theta}(x))_x=\boldsymbol{0}, \tag{1}$$

where $\boldsymbol{u}(x, t)=(u_1(x, t), u_2(x, t), \ldots, u_m(x, t))^{\mathrm{T}}$ is a solution vector, $\boldsymbol{\theta}(x)=(a(x), b_1(x), \ldots, b_m(x))^{\mathrm{T}}$ denotes all inhomogeneous factors on the road, and $\boldsymbol{f}(\boldsymbol{u}, \boldsymbol{\theta}(x))=(f_1(\boldsymbol{u}, \boldsymbol{\theta}(x)), f_2(\boldsymbol{u}, \boldsymbol{\theta}(x)), \ldots, f_m(\boldsymbol{u}, \boldsymbol{\theta}(x)))^{\mathrm{T}}$ is a vector-valued function. The model describes m types of vehicles in traffic flow with each having the density $u_l(x, t)=a(x)\rho_l(x, t)$, where $\rho_l(x, t)$ denotes the density per lane of the lth type and $a(x)$ represents the number of lanes. The velocity of the lth type of vehicle, v_l, is given by

$$\begin{gathered} v_l=b_l(x)v(\rho),\ v'(\rho)=\frac{\mathrm{d}v}{\mathrm{d}\rho}<0,\ b_l(x)=v_{l,\mathrm{f}}(x)\big/v_{\mathrm{f}}, \\ v_{\mathrm{f}}=\max_x \max_{1\le l\le m} v_{l,\mathrm{f}}(x), \end{gathered} \tag{2}$$

where $\rho=\sum_{l=1}^{m}\rho_l$ is the total density, $v(\rho)$ is a speed-density relationship, $v_{l,\mathrm{f}}(x)$ is the free flow (maximum) velocity of the lth type of vehicle, and v_{f} is the maximum of the free flow velocities. Accordingly, $\{b_l(x)\}_{l=1}^{m}$ reflect the velocity differences between m vehicle types, and $0\le b_l\le 1$.

Assume that $b_i<b_j$ holds for $i<j$. Then the eigenvalues $\{\lambda_l\}_{l=1}^{m}$ of the Jacobian $\boldsymbol{f}_u$ satisfy

$$\begin{aligned} &v_1+\sum_{l=1}^{m}\rho_l\frac{\partial v_l}{\partial\rho}<\lambda_1<v_1<\lambda_2<\cdots<v_{l-1}<\lambda_l<v_l \\ &<\cdots<v_{m-1}<\lambda_m<v_m,\ \text{ for } \boldsymbol{u}/a\in D, \end{aligned} \tag{3}$$

where $D=\left\{\boldsymbol{u}/a\middle|\rho_l>0;\ l=1,2,\cdots,m;\ \sum_{l=1}^{m}\rho_l<\rho_{\mathrm{jam}}\right\}$, and ρ_{jam} is the jam density. This equation indicates that the system is strictly hyperbolic in D. In this study we consider only the above case. The detailed structural properties of Eq. (3) were thoroughly discussed by Zhang *et al*. (2006a).

The MCLWR model on an inhomogeneous highway is important in many practical applications. For instance, the changes of $\boldsymbol{\theta}(x)$ reflect the decrease or increase in traffic capacity in many specific locations, such as on curves and near ramps. One particular example is to use $b_l=b_l(x, t)$ as a switch function in a traffic signal problem. This means all the coefficients in $\boldsymbol{\theta}$ may be discontinuous at the change. In this case, if the flux $\boldsymbol{f}(\boldsymbol{u}, \boldsymbol{\theta}(x))_x$ is also a discontinuous function, it is more difficult to develop numerical methods for these systems. Following Zhang *et al*. (2006b), the model (1)–(2) is rewritten in the 'standard' conservation form:

$$\boldsymbol{U}_t+\boldsymbol{F}_x=\boldsymbol{0}, \tag{4}$$

where $\boldsymbol{U}=(\boldsymbol{u}, \boldsymbol{\theta})^{\mathrm{T}}$ and $\boldsymbol{F}=\boldsymbol{f}((\boldsymbol{u}, \boldsymbol{\theta}), \boldsymbol{0})^{\mathrm{T}}$. The eigenvalues $\{\lambda_l\}_{l=1}^{m}$ of the Jacobian $\boldsymbol{F}_U$ also satisfy inequality (3), and the eigenvalues $\{\lambda_l\}_{l=m+1}^{2m+1}$ are equal to zero.

3 Numerical scheme

Based on the relaxation method approximation, the system (4) can be replaced by the relaxation system

$$\begin{cases}\boldsymbol{U}_t+\boldsymbol{V}_x=\boldsymbol{0},\\ \boldsymbol{V}_t+\boldsymbol{A}^2\boldsymbol{U}_x=-(\boldsymbol{V}-\boldsymbol{F}(\boldsymbol{U}))/\tau,\end{cases} \tag{5}$$

where $\boldsymbol{V}\in\mathbb{R}^{2m+1}$, $\boldsymbol{A}=\mathrm{diag}\{a_1, a_2, \ldots, a_{2m+1}\}$ is a positive diagonal matrix, and $\tau>0$ is a small constant called the relaxation rate. The above relaxation system (5) has characteristic variables given by

$$\boldsymbol{V}\pm\boldsymbol{A}\boldsymbol{U}. \tag{6}$$

The relaxation system (5) can be solved without employing Riemann solvers. This is the main advantage of introducing system (5). Moreover, the solution of Eq. (5) tends to the solution of the original problem as $\tau\to0$, provided that the following sub-characteristic condition holds:

$$-a\le\lambda\le a, \tag{7}$$

where $a=\max\{a_1, a_2, \ldots, a_{2m+1}\}$ and λ is an arbitrary eigenvalue of the Jacobian $\boldsymbol{F}_U$.

3.1 Space discretization

For simplicity, let us consider a uniform spatial grid $x_\beta=\beta$. We use $\boldsymbol{U}_j(t)=\frac{1}{\Delta x}\int_{I_j}\boldsymbol{U}(x,t)\mathrm{d}x$ and $\boldsymbol{U}_{j+\frac{1}{2}}(t)$ to represent the approximate cell average of the variable $\boldsymbol{U}$ in $I_j=[x_{j-\frac{1}{2}}, x_{j+\frac{1}{2}}]$ and the approximate point value of $\boldsymbol{U}$ at $(x_{j+\frac{1}{2}}, t)$, respectively.

The spatial and time discretization for the relaxation system (5) can be separated by using the 'method-of-lines' approach (Jin and Xin, 1995). Keeping the time continuous, one can obtain the spatial discretization of Eq. (5) given by

$$\begin{cases}\dfrac{\mathrm{d}}{\mathrm{d}t}\boldsymbol{U}_j+\dfrac{1}{\Delta x}(\boldsymbol{V}_{j+\frac{1}{2}}-\boldsymbol{V}_{j-\frac{1}{2}})=\boldsymbol{0},\\ \dfrac{\mathrm{d}}{\mathrm{d}t}\boldsymbol{V}_j+\dfrac{1}{\Delta x}\boldsymbol{A}^2(\boldsymbol{U}_{j+\frac{1}{2}}-\boldsymbol{U}_{j-\frac{1}{2}})=-\dfrac{1}{\tau}(\boldsymbol{V}_j-\boldsymbol{F}(\boldsymbol{U})_j).\end{cases} \tag{8}$$

We now consider the relaxed system resulting from the semi-discrete formulation (8) in the limit $\tau\to0$, which is given by

$$\frac{\mathrm{d}}{\mathrm{d}t}\boldsymbol{U}_j+\frac{1}{\Delta x}(\boldsymbol{V}_{j+\frac{1}{2}}-\boldsymbol{V}_{j-\frac{1}{2}})=\boldsymbol{0},\ \ \boldsymbol{V}_j=\boldsymbol{F}(\boldsymbol{U}_j). \tag{9}$$

The space discretization of a relaxed scheme consists of two steps. The first step is to build a piecewise reconstruction from the given cell-averages $\{\boldsymbol{U}_j\}$ resulting in

$$\tilde{\boldsymbol{U}}(x)=\sum\nolimits_j\boldsymbol{P}_j(x;\boldsymbol{U})\chi_j(x). \tag{10}$$

Here $\boldsymbol{P}_j(x;\boldsymbol{U})$ is a polynomial vector defined in I_j and χ_j is the characteristic function of the interval I_j. Given such a reconstruction, the point-values of $\tilde{\boldsymbol{U}}$ at the interface points are denoted by $\boldsymbol{U}^-_{j+\frac{1}{2}}=\boldsymbol{P}_j(x_{j+\frac{1}{2}};\boldsymbol{U})$ and $\boldsymbol{U}^+_{j-\frac{1}{2}}=\boldsymbol{P}_j(x_{j-\frac{1}{2}};\boldsymbol{U})$. To achieve high-order approximations, one can use higher-order non-oscillatory reconstructions such as essentially non-oscillatory (ENO), WENO, and central-WENO reconstructions. In this paper, we use an improved fifth-order WENO reconstruction (Borges *et al*., 2008).

Based on this reconstruction, the computation of $\boldsymbol{U}^-_{j+\frac{1}{2}}$ yields

$$U^-_{j+\frac{1}{2}}=P_j(x_{j+\frac{1}{2}};\boldsymbol{U})=\sum_{r=0}^{2}\omega_r Q^{(r)}_{j+\frac{1}{2}}, \tag{11}$$

where $U^-_{j+\frac{1}{2}}$ and P_j are the kth components of $\boldsymbol{U}^-_{j+\frac{1}{2}}$ and $\boldsymbol{P}_j$, respectively. The $Q^{(r)}_{j+\frac{1}{2}}$ have the form

$$\begin{cases}Q^{(0)}_{j+\frac{1}{2}}=\dfrac{1}{3}U_j+\dfrac{5}{6}U_{j+1}-\dfrac{1}{6}U_{j+2},\\ Q^{(1)}_{j+\frac{1}{2}}=-\dfrac{1}{6}U_{j-1}+\dfrac{5}{6}U_j+\dfrac{1}{3}U_{j+1},\\ Q^{(2)}_{j+\frac{1}{2}}=\dfrac{1}{3}U_{j-2}-\dfrac{7}{6}U_{j-1}+\dfrac{11}{6}U_j.\end{cases} \tag{12}$$

The weights ω_r are defined by

$$\omega_r=\frac{\alpha_r}{\sum_{l=0}^{2}\alpha_l},\ \alpha_r=C_r\left(1+\frac{\eta_5}{\mathrm{IS}_r+\varepsilon}\right),\ r=0,\ 1,\ 2, \quad (13)$$

where C_0=3/10, C_1=3/5, C_2=1/10, and ε is a small number. In our numerical simulations, ε is set to 10^{-10}. The smoothness indicators are given by

$$\begin{cases}\mathrm{IS}_0=\dfrac{13}{12}(U_j-2U_{j+1}+U_{j+2})^2+\dfrac{1}{4}(3U_j-4U_{j+1}+U_{j+2})^2,\\ \mathrm{IS}_1=\dfrac{13}{12}(U_{j-1}-2U_j+U_{j+1})^2+\dfrac{1}{4}(U_{j-1}-U_{j+1})^2,\\ \mathrm{IS}_2=\dfrac{13}{12}(U_{j-2}-2U_{j-1}+U_j)^2+\dfrac{1}{4}(U_{j-2}-4U_{j-1}+3U_j)^2.\end{cases} \quad (14)$$

The expression of η_5 in terms of the smoothness indicators is

$$\eta_5=\left|\mathrm{IS}_0-\mathrm{IS}_2\right|. \quad (15)$$

The computation of $\boldsymbol{U}^{+}_{j-\frac{1}{2}}$ is obtained by symmetry. In a similar way, we can obtain the reconstructions $\boldsymbol{P}_j(x;\ \boldsymbol{V}+\boldsymbol{AU})$ and $\boldsymbol{P}_j(x;\ \boldsymbol{V}-\boldsymbol{AU})$.

The second step is to use these reconstructions to discretize the characteristic variables (6), which yields

$$\begin{cases}(V+a_kU)_{j+\frac{1}{2}}=(V+a_kU)^{-}_{j+\frac{1}{2}}=P_j(x_{j+\frac{1}{2}};\ \boldsymbol{V}+a_k\boldsymbol{U}),\\ (V-a_kU)_{j+\frac{1}{2}}=(V-a_kU)^{+}_{j+\frac{1}{2}}=P_{j+1}(x_{j+\frac{1}{2}};\ \boldsymbol{V}-a_k\boldsymbol{U}),\end{cases} \quad (16)$$

where V, $V+a_kU$, and $V-a_kU$ are the kth components of $\boldsymbol{V}$, $\boldsymbol{V}+\boldsymbol{AU}$, and $\boldsymbol{V}-\boldsymbol{AU}$, respectively. A straightforward calculation based on Eq. (16) gives

$$V_{j+\frac{1}{2}}=\frac{1}{2}\left(P_j(x_{j+\frac{1}{2}};\ \boldsymbol{V}+a_k\boldsymbol{U})+P_{j+1}(x_{j+\frac{1}{2}};\ \boldsymbol{V}-a_k\boldsymbol{U})\right). \quad (17)$$

Here $V_{j+\frac{1}{2}}$ is the kth component of $\boldsymbol{V}_{j+\frac{1}{2}}$.

3.2 Time discretization

Based on the spatial discretization, we obtain the semi-discrete formulation rewritten in a common ordinary differential equation form:

$$\frac{\mathrm{d}}{\mathrm{d}t}\boldsymbol{U}_j=\boldsymbol{L}(\boldsymbol{U}), \quad (18)$$

where $\boldsymbol{L}(\boldsymbol{U})=(\boldsymbol{V}_{j+\frac{1}{2}}-\boldsymbol{V}_{j-\frac{1}{2}})/\Delta x$. For time discretization, we use the third-order SSP Runge-Kutta scheme (Gottlieb *et al*., 2001):

$$\begin{cases}\boldsymbol{U}^{(1)}=\boldsymbol{U}^n+\Delta t\cdot\boldsymbol{L}(\boldsymbol{U}^n),\\ \boldsymbol{U}^{(2)}=\dfrac{3}{4}\boldsymbol{U}^n+\dfrac{1}{4}\boldsymbol{U}^{(1)}+\dfrac{1}{4}\Delta t\cdot\boldsymbol{L}(\boldsymbol{U}^{(1)}),\\ \boldsymbol{U}^{n+1}=\dfrac{1}{3}\boldsymbol{U}^n+\dfrac{2}{3}\boldsymbol{U}^{(2)}+\dfrac{2}{3}\Delta t\cdot\boldsymbol{L}(\boldsymbol{U}^{(2)}).\end{cases} \quad (19)$$

The Courant-Friedrichs-Lewy (CFL) number is defined by

$$\mathrm{CFL}=\max_l\left(a_l\frac{\Delta t}{\Delta x}\right)\le 1.0. \quad (20)$$

The parameters a_l for $1\le l\le 2m+1$ are chosen according to inequality (7). For example, a simple choice is to take $a_l=\alpha$ for $1\le l\le 2m+1$. Here and below, we take $\alpha=\max\left(\left|v_1+\sum_{l=1}^{m}\rho_l\dfrac{\partial v_l}{\partial\rho}\right|,\ \left|v_m\right|\right)$. Other choices can be made as long as condition (7) holds.

4 Numerical examples

We choose several numerical examples studied by Zhang *et al.* (2006b) to validate the performance of the present scheme for the MCLWR model on an inhomogeneous highway.

The velocities of Eq. (2) are set to be linear (Drake *et al*., 1967):

$$v(\rho)=v_{\mathrm{f}}(1-\rho/\rho_{\mathrm{jam}}).$$

In all illustrations, the variables of ρ_l and ρ are scaled by ρ_{jam}, and the computational domain $(0, L)$ is scaled to be $(0, 1)$. Moreover, a variable is non-dimensional if it is not followed by its unit.

4.1 Resolution of the waves

The first example involves three types of vehicles. The computational parameters are

L=8000 m, T=400 s, v_f=20 m/s, Δx=20 m,
$b_1(x)$=0.5, $b_2(x)$=0.75, $b_3(x)$=1.0, CFL=0.2,

where T is the computation time. Two scaled initial data sets are chosen as follows:

$$(1)\ (a,\rho_1,\rho_2,\rho_3)=\begin{cases}(3,0.2,0.15,0.05), & x\le 0.3,\\ (1,0.05,0.15,0.2), & x>0.3.\end{cases}$$

$$(2)\ (a,\rho_1,\rho_2,\rho_3)=\begin{cases}(2,0.3,0.25,0.15), & x\le 0.5,\\ (3,0.15,0.2,0.25), & x>0.5.\end{cases}$$

For these two cases, the solutions of total density consist of three shocks, a contact, and a rarefaction. Figs. 1 and 2 show the results for initial data sets (1) and (2), respectively. The numerical results are plotted together with reference solutions, computed using our scheme with 1600 grid points. The computed results show good agreement with the reference solutions, and the shock and rarefaction waves are well resolved by the present method. For initial data sets (1) and (2), we use $a_l=\alpha$ for l=1, 2, …, 7.

4.2 Traffic signal control problem

The second example is a traffic signal control problem. In this problem the functions of $\boldsymbol{\theta}$ are also temporal. This is very common in traffic problems, and signal control is a typical example of the extension (Zhang *et al*., 2006b). At the stop line, which is near x=0.35 on a road that is 1200 m long, the traffic light changes from green to red (at t=0) for 30 s and back to green for another 30 s. The $b_l(x)$ are taken as

$$(b_1,b_2,b_3)=\begin{cases}(0,0,0), & \text{if } 0.34<x<0.36\\ & \text{and } 0<t-60[t/60]\le 30 \text{ s},\\ (0.5,0.75,1), & \text{otherwise.}\end{cases}$$

The initial conditions are

$$\boldsymbol{u}(x,0)/a=[0.05,\ 0.25,\ 0.1]^{\mathrm{T}},$$

where $a(x)$ is assumed to be constant. Figs. 3 and 4 show the results of density of all classes and total density, respectively. The solution is computed up to

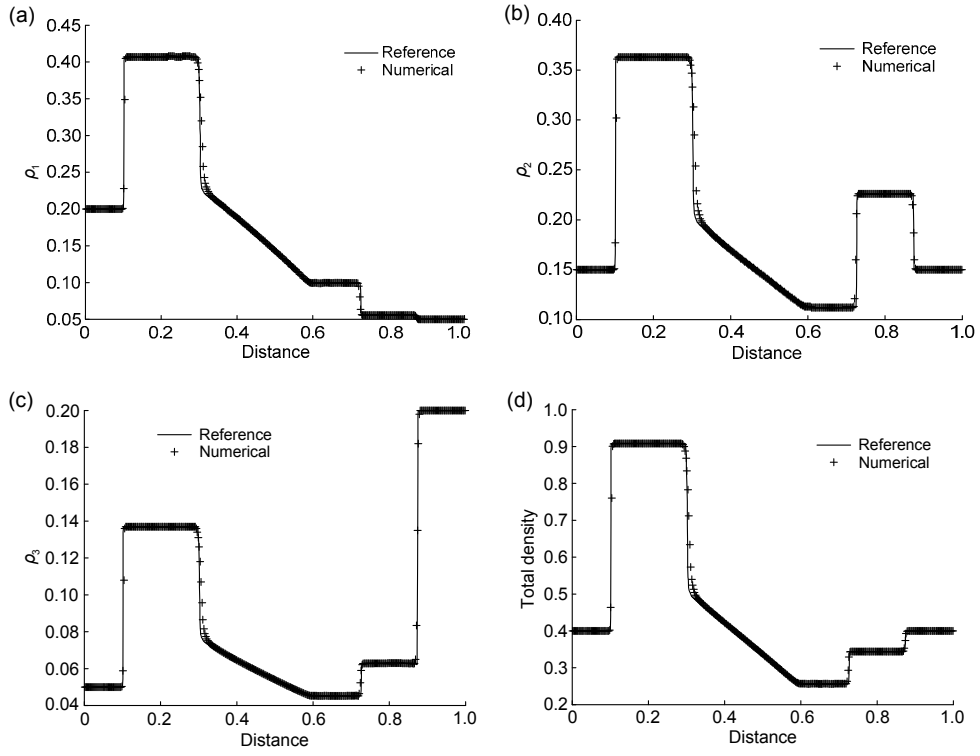

Fig. 1 Comparison between the numerical results and the reference solutions for initial data set (1)
(a) Density ρ_1; (b) Density ρ_2; (c) Density ρ_3; (d) Total density

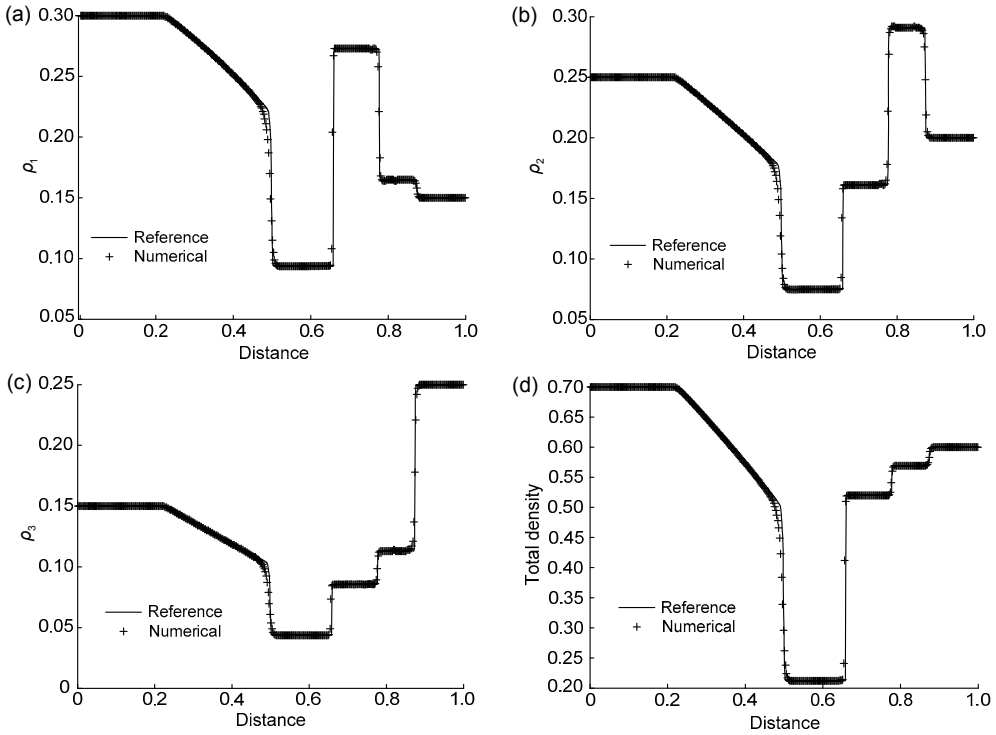

Fig. 2 Comparison between the numerical results and the reference solutions for initial data set (2)
(a) Density ρ_1; (b) Density ρ_2; (c) Density ρ_3; (d) Total density

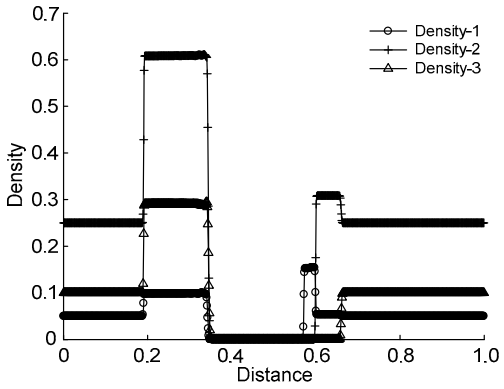

Fig. 3 Densities of all classes at t=30 s in the traffic signal control problem

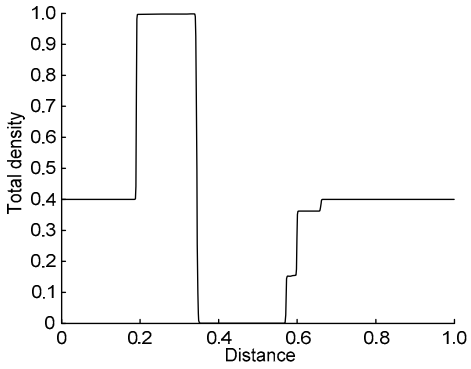

Fig. 4 Total density at t=30 s in the traffic signal control problem

t=30 s, using 800 cells. There is a waiting queue on the left-hand side of the stop line, and during the interval this queue propagates backwards before the green signal. Moreover, the total density reaches its maximum value in the queue, and three shocks appearing on the right-hand side of the stop line represent overtaking between the three types of vehicles. In this case we take a_l=α for l=1, 2, …, 7 and CFL=0.45. Using the same parameters, the whole evolution of the total density in a period of 60 s is shown in Fig. 5.

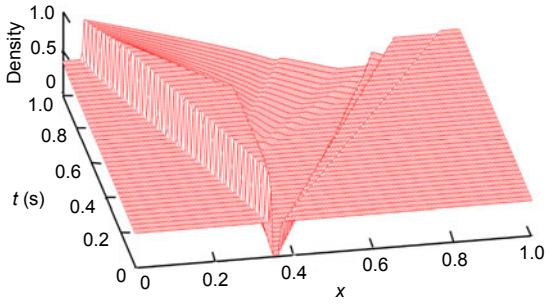

Fig. 5 Change of total density at t=60 s in the traffic signal control problem for three types of vehicles

The next case involves five types of vehicles. The $b_l(x)$ are given by

$$(b_1,b_2,b_3,b_4,b_5)=\begin{cases}(0,0,0,0,0), & \text{if } 0.34<x<0.36\\ & \text{and } 0<t-60[t/60]\le 30\text{ s},\\ (0.6,0.7,0.8,0.9,1), & \text{otherwise.}\end{cases}$$

The initial data are

$$\boldsymbol{u}(x,0)/a=[0.15,\ 0.05,\ 0.1,\ 0.05,\ 0.05]^{\mathrm{T}}.$$

Fig. 6 shows the change of total density at t=60 s. Five small staircases relative to five types of vehicles can be observed. These staircases are actually shocks. The result suggests that the present scheme can be used to reproduce queuing and dissipation in the presence of more types of vehicles. In this case we use $a_l=\alpha$ for l=1, 2, …, 11 and CFL=0.45.

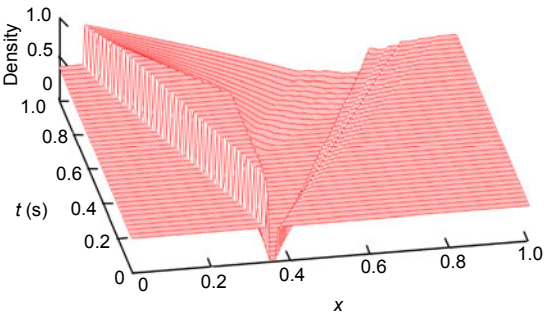

Fig. 6 Change of total density at t=60 s in the traffic signal control problem for five types of vehicles

5 Conclusions

In this paper we have presented a high-resolution relaxed scheme for an MCLWR traffic flow model on an inhomogeneous highway. We have incorporated an improved WENO reconstruction into a relaxation approximation to improve the resolution and accuracy. The resulting method was tested on two examples and produced satisfactory results.

References

Banda, M.K., 2005. Variants of relaxed schemes and two-dimensional gas dynamics. *J. Comput. Appl. Math.*, **175**(1):41-62. [doi:10.1016/j.jcam.2004.06.008]

Banda, M.K., 2009. Non-oscillatory relaxation schemes for one-dimensional ideal magnetohydrodynamic equations. *Nonl. Anal. Real World Appl.*, **10**(6):3345-3352. [doi:10.1016/j.nonrwa.2008.09.024]

Banda, M.K., Seaïd, M., 2005. Higher-order relaxation schemes for hyperbolic systems of conservation laws. *J. Numer. Math.*, **13**(3):171-196. [doi:10.1515/156939505774286102]

Banda, M.K., Seaïd, M., 2007. Relaxation WENO schemes for multidimensional hyperbolic systems of conservation laws. *Numer. Methods Part. Differ. Equat.*, **23**(5):1211-1234. [doi:10.1002/num.20218]

Borges, R., Carmona, M., Costa, B., Don, W.S., 2008. An improved weighted essentially non-oscillatory scheme for hyperbolic conservation laws. *J. Comput. Phys.*, **227**(6):3191-3211. [doi:10.1016/j.jcp.2007.11.038]

Bürger, R., García, A., Karlsen, K.H., Towers, J.D., 2008. A family of numerical schemes for kinematic flows with discontinuous flux. *J. Eng. Math.*, **60**(3-4):387-425. [doi:10.1007/s10665-007-9148-4]

Chen, J.Z., Shi, Z.K., 2006. Application of a fourth-order relaxation scheme to hyperbolic systems of conservation laws. *Acta Mech. Sin.*, **22**(1):84-92. [doi:10.1007/s10409-005-0079-x]

Chen, J.Z., Shi, Z.K., Hu, Y.M., 2009. A relaxation scheme for a multi-class Lighthill-Whitham-Richards traffic flow model. *J. Zhejiang Univ.-Sci. A*, **10**(12):1835-1844. [doi:10.1631/jzus.A0820829]

Drake, J.S., Schofer, J.L., May, A.D., 1967. A statistical analysis of speed density hypothesis. *Highway Res. Rec.*, **154**:53-87.

Gottlieb, S., Shu, C.W., Tadmor, E., 2001. Strong stability preserving high order time discretization methods. *SIAM Rev.*, **43**(1):89-112. [doi:10.1137/S003614450036757X]

Jin, S., Xin, Z., 1995. The relaxation schemes for systems of conservation laws in arbitrary space dimensions. *Commun. Pure Appl. Math.*, **48**(3):235-276. [doi:10.1002/cpa.3160480303]

Lighthill, M.J., Whitham, G.B., 1955. On kinematic waves (II): a theory of traffic flow on long crowed roads. *Proc. R. Soc. Ser. A*, **229**(1178):317-345. [doi:10.1098/rspa.1955.0089]

Ngoduy, D., 2010. Multiclass first-order modelling of traffic networks using discontinuous flow-density relationships. *Transportmetrica*, **6**(2):121-141. [doi:10.1080/18128600902857925]

Richards, P.I., 1956. Shock waves on the highway. *Oper. Res.*, **4**(1):42-51. [doi:10.1287/opre.4.1.42]

Wong, G.C.K., Wong, S.C., 2002. A multi-class traffic flow model—an extension of LWR model with heterogeneous drivers. *Transp. Res. Part A*, **36**(9):827-841. [doi:10.1016/S0965-8564(01)00042-8]

Zhang, M.P., Shu, C.W., Wong, G.C.K., Wong, S.C., 2003. A weighted essentially non-oscillatory numerical scheme for a multi-class Lighthill-Whitham-Richards traffic flow model. *J. Comput. Phys.*, **191**(2):639-659. [doi:10.1016/S0021-9991(03)00344-9]

Zhang, P., Liu, R.X., Wong, S.C., Dai, S.Q., 2006a. Hyperbolicity and kinematic waves of a class of multi-population partial differential equations. *Eur. J. Appl. Math.*, **17**(2):171-200. [doi:10.1017/S095679250500642X]

Zhang, P., Wong, S.C., Shu, C.W., 2006b. A weighted essentially non-oscillatory numerical scheme for a multi-class traffic flow model on an inhomogeneous highway. *J. Comput. Phys.*, **212**(2):739-756. [doi:10.1016/j.jcp.2005.07.019]

Zhang, P., Wong, S.C., Xu, Z.L., 2008. A hybrid scheme for solving a multi-class traffic flow model with complex wave breaking. *Comput. Methods Appl. Mech. Eng.*, **197**(45-48):3816-3827. [doi:10.1016/j.cma.2008.03.003]